

A computational modelling approach to investigate alpha rhythm slowing associated with Alzheimer's Disease

Basabdatta Sen Bhattacharya, Damien Coyle and Liam Maguire

Abstract Attenuation of power in the alpha band (8–13 Hz) of Electroencephalography (EEG) is identified as a hallmark symptom of Alzheimer's Disease (AD). There is general agreement in existing literature that the thalamocortical circuitry play a key role in generation of alpha rhythms. Our research is to gain a better understanding of the cause of alpha rhythm slowing in the thalamocortical circuitry, which in turn might help in early detection of Alzheimer's Disease. We adopt a computational approach and base our work on a classic computational model of the thalamocortical circuitry associated with the generation of alpha rhythms proposed by Lopes Da Silva. In this work, we use the model to do a preliminary study on the power spectrum of the alpha rhythms by varying model parameters corresponding to inhibitory and excitatory synaptic activity. We observe that an increased inhibitory synaptic activity in the network leads to a decrease in the power of the upper alpha frequency band (11–13 Hz) and an increase in that of the lower alpha frequency band (8–10 Hz). Thus we observe an overall slowing of alpha rhythm corresponding to an increase in the inhibitory synaptic activity in the thalamocortical circuitry.

1 Introduction

One of the major challenges in the current treatment of Alzheimer's Disease (AD) is its early diagnosis. Pathological changes in the brain associated with AD are now well known as are the cognitive and behavioural changes in patients affected with AD. Yet, there is little therapeutic success in these cases. One of the main reasons

Basabdatta Sen Bhattacharya
University of Ulster, ISRC, Magee e-mail: bs.bhattacharya@ulster.ac.uk

Damien Coyle
University of Ulster, ISRC, Magee e-mail: dh.coyle@ulster.ac.uk

Liam Maguire
University of Ulster, ISRC, Magee e-mail: lp.maguire@ulster.ac.uk

for this is that early clinical symptoms of AD cannot be distinguished from other forms of mental dementia related to advancing age. Moreover, such symptoms are often also associated with ageing of normal adults [17]. Distinct clinical symptoms specific to AD appear only when the brain has already undergone a major pathological degradation corresponding to an advanced state of the disease [7]. Therapies currently used are mainly to delay symptomatic degradation. It is strongly believed that early detection of AD might help in specifying drugs to delay the onset of the disease by even a decade, so much so that even possibilities of curing the disease are not completely ruled out [5, 7].

Diminished power in the alpha frequency band (8–13 Hz), commonly referred to in literature as ‘slowing’ of alpha rhythms, is identified as a definite marker in the EEG of AD patients [16, 4, 20]. Although such slowing of alpha rhythms are an indicator of underlying pathological aberration related with many neurological as well as psychological disorders [8, 14], early stage AD patients are ‘fairly’ distinguishable from a set of control patients and patients affected with mental depression with a correct classification rate of 77% and 72% respectively, albeit in a clinically restrained environment [16, 20]. Alpha rhythm slowing is also a distinct marker for patients with Mild Cognitive Impairment (MCI)¹ [1]—28.2% of MCI patients were detected with AD during a clinical follow-up after 14.8 months [19]. These findings provide support to the speculation that MCI may be a precursor to AD [1, 19]. The only significant difference observed between untreated AD patients and those treated with cholinesterase inhibitor is in the alpha frequency band [2]. Thus, a good understanding of the underlying cause of the diminishing power in the alpha band with MCI or AD may elucidate future therapeutic techniques as well as early diagnosis of AD.

There is now a general agreement in literature that the thalamocortical circuitry play a key role in the generation of alpha rhythms [3, 8, 10, 11]. In his seminal work on alpha rhythms in thalamocortical network of awake dogs, Lopes da Silva proposed that alpha rhythms are filter-like treatment of stochastic signals by groups of similar neuronal networks existing in different areas of the thalamus and the cortex [12]. To test this hypothesis, he proposed a computational model based on histological data obtained by Tombol during her Golgi studies on the thalamus of an adult cat [24]. He showed that the output of the model indeed oscillates at alpha rhythmic frequencies when stimulated with a random input [12]. A linear system analysis of the model was also presented as a platform for further investigation of the effects on the output rhythmic activity by varying the model parameters.

We start by validating the linear system representation of the computational model proposed in [12]. This is with a goal of studying the changes in alpha rhythm characteristics of the output voltage effected by varying the free parameters of the model and the significance and relation of the effects of such variation in understanding AD and its early diagnosis. In this work we present preliminary results by varying parameters related to inhibitory and excitatory synapses in the model. We observe that an increase in inhibitory synaptic activity diminishes the average power

¹ a clinical state between normal old age and mental dementia

in the upper alpha band (11–13 Hz) while power in the lower alpha band (8–10 Hz) is increased. Thus there is an overall slowing of alpha rhythms. Furthermore, we observe that variation in the excitatory synaptic activity does not affect this slowing. From this observation we speculate that the inhibitory thalamocortical pathway has an important functional role in slowing of alpha rhythms.

In Sect. 2, we present our validation of Lopes da Silva’s Alpha Rhythm model (ARm). In Sect. 3, we present our work based on the model and the results obtained thereof. We conclude by a discussion of our results in the context of AD and future directions in Sect. 4.

2 Validation of Alpha Rhythm model

In this section, we present a very brief biological background from Tombol’s work [24] which is the basis of the biological parameters used to design the ARm [12]. This is followed by a description of the model and our validation of the simulation results and the linear representation as was done by Lopes da Silva. It is worth mentioning here that the distributed-model of alpha rhythm was proposed and validated by Lopes da Silva with experimental results obtained from the thalamic and cortical areas of a dog in a relaxed-awake state [12]. In this paper we present validation of simulation results from the lumped-model version of the ARm.

2.1 *A brief biological background*

Based on Golgi studies on the thalamus of a well developed cat, Tombol observed that two typical kinds of nerve cell generally occur in all areas of the thalamus: the thalamocortical relay (TCR) neurons with large axons and internuncial (IN) neurons with short axons [24]. It is estimated that more than ten afferents from outside the thalamus project on to the dendrites of one TCR cell. Furthermore, these afferents make strong excitatory synapses on both TCRs and INs. The axons of the IN population also make strong synaptic contacts with the TCR dendrites. At a short distance from the axon hillock of many of the TCR cells, collaterals are seen to branch off from the axon.

Based on this biological data, Lopes da Silva considers two types of neuronal population in his model viz. the TCR and IN cells. The TCR is assumed to excite one or more IN neurons via a recurrent collateral of its axon. This is the feed-forward path of the model. The IN neurons in turn make inhibitory synaptic contacts with one or more TCR neurons, thus forming a negative feedback. As there are thought to be approximately 10 afferents converging on one TCR cell and assuming an action potential frequency of 20 pps (pulses per second) per fibre of the afferent connections to the TCR (based on relevant literature), it is assumed in the model that each TCR cell receives a 200 pps input. From the physiological dimensions provided by

Tombol, each TCR neuron in the model is designed to receive inhibitory input from 3 IN neurons. Due to a lack of available data, each IN neuron was assumed to receive input from 32 TCR neurons. The validation of the model simulation results in our work is discussed below.

2.2 Alpha Rhythm model

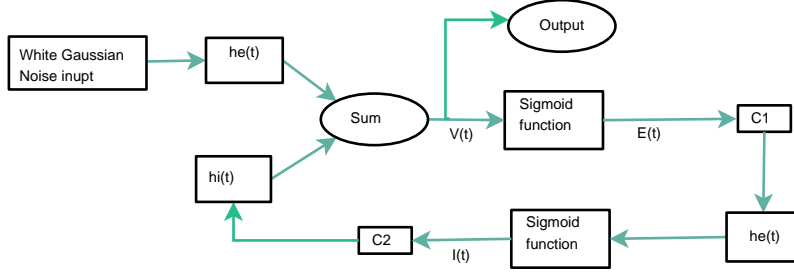


Fig. 1 The block diagram of Lopes Da Silva's lumped circuit model of alpha rhythm [12]. In this work, we have implemented the model using Simulink in Matlab as was done by Suffczynsky [23] (p. 26).

The functional block diagram of the ARm is shown in Fig. 1 [23]. The population of each type of neuron viz. TCR and IN are represented as single entities. Such a representation, termed as a 'lumped circuit model' by Freeman [6], is inspired by the pioneering works of Freeman in [6] and Wilson and Cowan in [25]. The input to the model is simulated by a Gaussian white noise having a mean P and a standard deviation of 1, the standard deviation representing the variation in the input spike frequency [23]. The excitatory post synaptic potential (EPSP) generated by a TCR neuron when depolarised by afferent signals is simulated by convolution of the input to the model by a positive wave function $h_e(t)$ shown in Fig. 2(a). Similarly, $h_i(t)$ corresponds to the inhibitory post synaptic potential (IPSP) generated by a IN neuron. Thus each TCR and IN neuron act as 'filters' of their respective inputs, the impulse function of the excitatory and inhibitory filters being $h_e(t)$ and $h_i(t)$ respectively and are defined in Eq. 1 [12]:

$$\begin{aligned} h_e(t) &= A[\exp(-a_1t) - \exp(-a_2t)] \\ h_i(t) &= B[\exp(-b_1t) - \exp(-b_2t)], \end{aligned} \quad (1)$$

where $A = 1.65mV$ and $B = 32mV$ represent the strength of the respective impulse functions while $a_1 = 55/sec$, $a_2 = 605/sec$, $b_1 = 27.5/sec$, $b_2 = 55/sec$ are the respective time constants [12, 23, 26]. C_1 in Fig. 1 represents the average excitatory input to one IN from the TCR population and is 32 as described in Sect. 2.1. Sim-

ilarly, $C_2 = 3$ represents the average inhibitory input that one TCR receives from the IN population [12]. $E(t)$ ($I(t)$) is the proportion of excitatory (inhibitory) cells firing per unit time in response to the average membrane potential $V(t)$; the relation is expressed as a sigmoid function and is defined as [21, 25, 26]:

$$\begin{aligned} E(t) &= g_0 \exp\{\gamma(V(t) - V_0)\}; \forall V \leq V_0 \\ E(t) &= g_0 [2 - \exp\{-\gamma(V(t) - V_0)\}]; \forall V > V_0, \end{aligned} \quad (2)$$

where V_0 is the threshold voltage, γ is the steepness parameter of the sigmoid function, g_0 and $2g_0$ are the maximum firing rates when $V(t) = V_0$ for the cases when $V \leq V_0$ and $V > V_0$ respectively. Here, $\gamma = 0.34/mV$, $g_0 = 25/sec$ and $V_0 = 7mV$ as in [21]. The summation unit may be thought to be resembling the post-synaptic somas of the excitatory and inhibitory neuronal population. The resulting average membrane potential $V(t)$ is the output of the system and simulates the EEG waveform studied on scalp of the awake humans in relaxed state and with eyes closed.

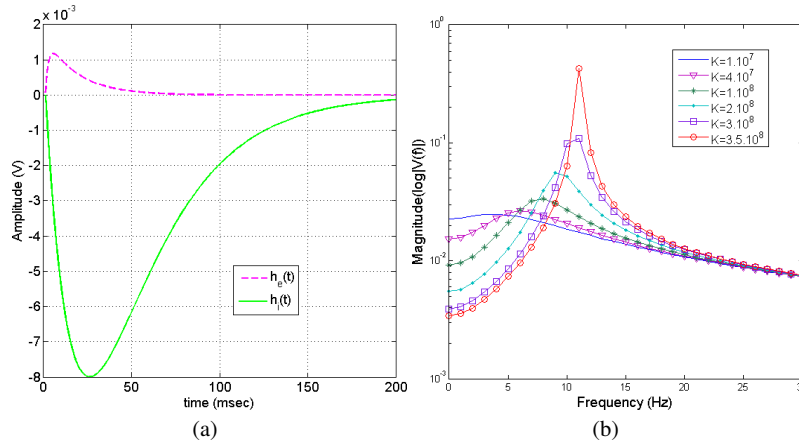


Fig. 2 (a) The excitatory and inhibitory impulse response functions of the TCR and IN neuronal population respectively [12, 26] (b) Power spectra of the transfer function with varying values of a control parameter K defined in Eq. 3.

2.3 Validating the model simulation results

In the steady state analysis presented by Lopes da Silva [12], the variation in the mean input to the TCR population is assumed to be small causing negligible variations in $V(t)$. Thus, for all practical purposes, $E(t)$ is assumed to be directly proportional to $V(t)$ and the sigmoid function in Eq. 2 is represented as the proportionality

constant q where $q = \frac{1}{2130}$. The transfer function of the linear analysis is:

$$\frac{V(s)}{P(s)} = \frac{A(a_2 - a_1)(s + b_1)(s + b_2)}{(s + a_1)(s + a_2)(s + b_1)(s + b_2) + K},$$

where $K = C_1 C_2 q^2 (a_2 - a_1)(b_2 - b_1) AB$ (3)

The power spectra of the transfer function is therefore independent of the mean input P . Furthermore, the spectrum is tuned to be alpha frequency selective with a narrow bandwidth by adjusting a control parameter K , which in turn is dependent on the impulse response as well as synaptic input parameters. We reproduce the power spectra of the transfer function as presented in Lopes da Silva's work [12] in Fig. 2(b). Observing the spectral characteristics of the transfer function, Lopes da Silva hypothesised that the evolution of posterior EEG with age from a predominantly low frequency signal to a signal having a high and narrow peak at around 10 Hz may depend on the number of synaptic inputs (C_1 and C_2) as well as on the amplitude of the synaptic potentials (A and B). Based on the simulation criteria, the change in the other parameters in K are assumed to be negligible.

3 Model set-up, analysis and results

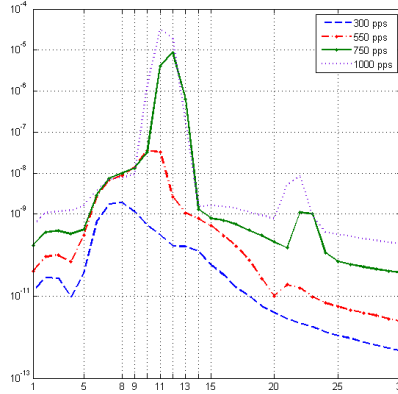


Fig. 3 The power spectra corresponding to average membrane potential output $V(t)$ of the ARm when the value of input P is 300, 550, 750 and 1000 pps. A distinct peak power at 12 Hz is observed when P has values nearer to 750 pps. The total power in the alpha band (8–13 Hz) does not increase considerably if P is increased from 750 pps to 1000 pps. (pps:pulses per second)

We base our work on the power spectrum of the output membrane potential V rather than that of the transfer function as presented in Sect. 2.3. Thus, the power spectrum in our work has a dependency on the input P . Moreover, we use the non-

linear sigmoid function as defined in Eq. 2. This is a different treatment of the model than in Lopes da Silva's work [12].

Figure 3 presents the power spectra of $V(t)$ corresponding to values of $P=300$, 550, 750 and 1000 pps chosen randomly at approximately equal intervals. This range of values for P is similar to those considered by Stam et al for a nonlinear dynamical analysis of the model [21]. We observe that at $P=750$ pps, the output voltage spectrum has a peak at 12 Hz and a narrow bandwidth spanning the alpha band (8–13 Hz). The overall power in the alpha band is considerably increased than those at $P=300$ and 500 pps. Furthermore, there is no remarkable change in the peak power or the bandwidth with $P=1000$ pps. In this work, we take the mean of our noisy input as $P=750$ pps. All the simulations are run on Simulink in Matlab and the output voltage is generated in real time. The total simulation time is 4 sec with a discrete time-step of 4 msec.

3.1 Results

The objective is to observe the power-spectral behaviour of the model by varying the parameters C_1 and C_2 related to the excitatory and inhibitory synaptic inputs respectively. We start by varying the value of C_2 from 1 to 5 in steps of unity while keeping C_1 constant at 32. For each value of C_2 , the simulation is run 10 times. The output voltage varies in each run because of the random nature of the noisy input. The power spectra of the output voltage for each run is obtained using a Welch's periodogram in Matlab with segment length of 1 sec, resolution of 1 Hz, and Hanning windowing with 50% overlap [4]. The average power over the 10 trials is then obtained for each value of C_2 and is shown in Fig. 4(a). We observe that as inhibition is increased by increasing C_2 , the power in the lower alpha band (8–10 Hz) is increased whereas that in the upper alpha band (11–13 Hz) is decreased. The mean power in each band for the values of C_2 are shown in Fig. 4(b). Thus we may say that the overall power in the alpha band decreases with an increase in inhibitory input. A one-way repeated measures analysis of variance (ANOVA) indicates that the difference in band powers given by the model are significant ($p \ll 0.001$). Furthermore, in Figs. 4(a) and 4(b), we observe distinct low frequency characteristics of the spectra for values of $C_2 < 3$. This agrees with the spectra in Fig. 2(b) which shows low-pass filter characteristics for values of K less than that corresponding to $C_2 = 3$ as discussed in Sect. 2.3. It was speculated that this phenomena may be an attribution of advancing age [12]. Figure 4(c) shows the power spectra for each value of C_2 which agrees with our observation of diminishing alpha band power with increasing inhibition.

To study the effect of the excitatory circuitry on alpha band slowing, we vary C_1 over a range of 10–50 so that the ratio $C_2 : C_1$ stays $\simeq 10$ as was taken originally in the model ($\frac{C_1}{C_2} = \frac{32}{3} \simeq 10$). For each value of C_1 , we vary the inhibitory synaptic parameter C_2 over the range 1–5 in a similar way as is done above. We observe an overall slowing of alpha rhythm, with a decrease in power for the upper alpha

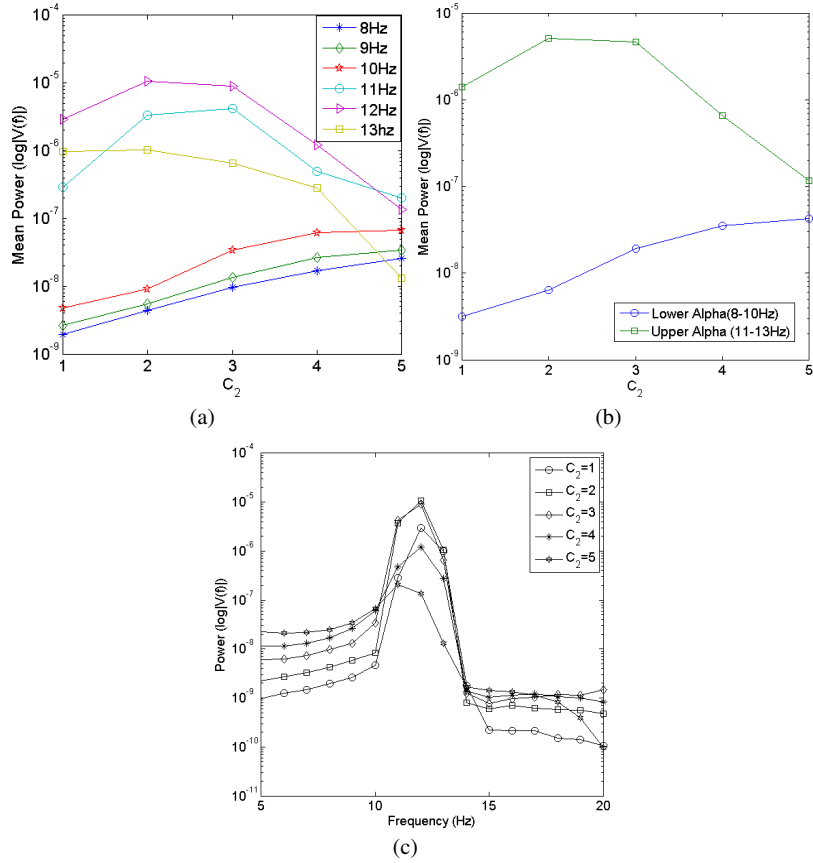


Fig. 4 (a) Average power of individual frequencies within the alpha band for different values of C_2 representing variations in inhibitory synaptic activity in the feedback path of the ARM. The excitatory synaptic activity parameter C_1 is kept constant at 32. (b) Average power in the lower alpha band (8–10 Hz) and upper alpha band (11–13 Hz) with varying values of C_2 when $C_1 = 32$. (c) Power spectrum of the output of the model corresponding to a constant value of $C_1 = 32$ and taking $C_2 = 1, 2, 3, 4$ and 5.

band frequencies and an increase in power for the lower alpha band frequencies as inhibition is increased. However, the power drop in the 12 Hz band with increased inhibitory activity (C_2) is relatively sharp for lower values of excitatory activities (C_1). We are currently carrying out further studies on this aspect. Overall, the variation of C_1 has a negligible effect on the power spectrum shift in alpha rhythms. The variation of power at each band within the alpha region for values of $C_1 = 20$ and $C_1 = 40$ are shown in Figs. 5(a) and 5(b). These figures are similar to Fig. 4(a) where alpha rhythm slowing was observed for $C_1 = 32$. The relative characteristics of the plots showing alpha rhythm slowing in Figs. 4(a), 5(a) and 5(b) are consistent for

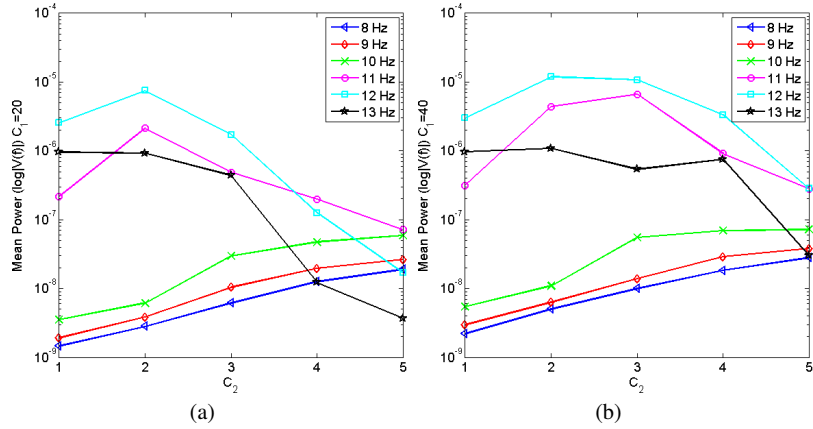


Fig. 5 Average power of individual frequencies within the alpha band for different values of C_2 representing variations in inhibitory synaptic activity in the feedback path of the ARm when (a) $C_1 = 20$ and (b) $C_1 = 40$, where C_1 represents the excitatory synaptic activity in the ARm.

$C_1 \leq 32$. In the next Section, we discuss the results presented here in the context of AD.

4 Discussion and future work

In this work, we have validated the simulation of a basic and simplified model of the thalamocortical circuit proposed for simulating alpha rhythmic activity of human EEG and have applied this model to assess dynamical changes observed in the EEG of AD patients. The power spectra of the output potential of the model shows high peak with a narrow bandwidth at around 12 Hz, thus mimicking alpha rhythms in EEG. We are interested in the change in behaviour, if any, of the power spectra of the output potential by varying parameters related to number of synaptic inputs.

From results presented in Sect. 3, we observe a slowing of alpha rhythm with the increase in the inhibitory synaptic activity. Furthermore, we observe no change in this characteristic when we vary the values of the parameter associated with excitatory synaptic activity. Thus, the inhibitory circuit seems to play a decisive role in the slowing of alpha rhythm. It is now well known that the primary inhibitory neurotransmitters in the mammalian brain is GABA. The long duration of $GABA_B$ associated IPSP is known to have a slowing effect on EEG rhythms [13, 23]. Furthermore, the relative effect of Alzheimer's Disease (AD) on GABAergic neurotransmitters is known to be negligible when compared to that on glutamatergic or cholinergic systems [18]. From the results presented in this work, we speculate that a deterioration in the excitatory synaptic pathway in AD gives rise to an imbalance in the excitatory and inhibitory neurotransmitters in a feedback system such as the thalamocortical

circuitry. This would provide a bias in the system towards an increased inhibitory activity, which in turn would affect the alpha rhythmic activity. Recent research on effects of AD on hippocampal inhibitory circuit speculates that the relative sparing of GABAergic systems by AD progression may be due to the increased synthesis of $GABA_A$ neurotransmitters in hippocampal neurons as a compensatory mechanism and adaptation against deterioration of the hippocampal inhibitory circuitry [18]. Such an argument may also be part of the inhibitory changes in the thalamocortical circuitry. Until recently, there was no definite evidence of physiological deterioration and effects of AD on the thalamus. However atrophy in thalamus related to (Mild Cognitive Impairment) MCI and AD has now been reported [9]. It is thus possible that a compensatory mechanism involving adaptations in the GABAergic system is also in play in the thalamocortical circuitry in AD whereby synthesis of GABA neurotransmitters by surviving cells is increased. Our findings presented in this work provide evidence to support this hypothesis.

The Alpha Rhythm model (ARm) validated and presented in this work provides a useful ‘starting point’ in our endeavour to understand the pathological origins of the changes in alpha rhythm as well as other brain rhythms associated with AD. The simplicity of the model makes it a popular basis for computational approaches in the study of EEG changes related to neurological disorders like Epilepsy and non-linear neuronal dynamics in thalamocortical circuitry [15, 21, 23, 26]; subsequently, the model was further developed in these works for enhanced biological plausibility. Indeed, the biological relevance of the model in current research seems to be its primary limitation. More recent research has revealed that Tombol’s Golgi study and the assumptions thereafter regarding the feedback mechanism of the internuncial (IN) neurons on the thalamocortical relay (TCR) neurons are flawed; however, it is demonstrated that IN neurons are indeed GABAergic in nature [22]. Thus the inherent inhibitory property of the feedback loop used in the model is not affected by these new findings. It is now believed that there is strong involvement of circuitry comprising of the thalamocortical, corticocortical and reticular nucleus (RE) in the generation of the different categories of brain rhythm [11, 13]. Although cells found in the RE do not resemble the IN neurons, they are GABAergic. Again, if the simplified single loop feedback circuit of the model is thought to comprise of RE neuronal populations, the nature of the connection would still be inhibitory. This justifies using the model for preliminary work on computational approaches to alpha rhythms in EEG.

Currently, we are investigating further into the behaviour of the excitatory thalamocortical circuitry to alpha rhythm slowing and its implications in the context of AD. As future work, we propose to extend the model on the lines of those presented in Suffczynsky’s work [23] for investigating event related synchronisation (ERS) and desynchronisation (ERD) observed in the alpha band rhythm and the association with AD. We also plan to investigate theta rhythms in AD using a similar computational approach.

References

1. Babiloni C et al (2009) Hippocampal volume and cortical sources of EEG alpha rhythms in mild cognitive impairment and Alzheimer disease. *Neuroim* 44:123–135
2. Basar E, Guntekin B (2008) A review of brain oscillations in cognitive disorders and the role of neurotransmitters. *Brain Res* 1235:172–193
3. Basar E et al (1997) Alpha oscillations in brain functioning: an integrative theory. *Int Jour Psychophysiol* 26:5–29
4. Canterro JL et al (2009) Functional integrity of thalamocortical circuits differentiates normal aging from Mild Cognitive Impairment. *Hum Br Map* 30:3944–3957
5. Cummings JL et al (1998) Alzheimer's disease: Etiologies, pathophysiology, cognitive reserve, and treatment opportunities. *Neurol* 51(Suppl 1):S2–S17
6. Freeman WJ (1975) Mass action in the nervous system. Academic Press, New York
7. Geula C (1998) Abnormalities of neural circuitry in Alzheimer's disease. *Neurol* 51(Suppl 1):S18–S29
8. Hughes SW, Crunelli V (2005) Thalamic mechanisms of EEG alpha rhythms and their pathological implications. *Neurosci*, doi: 10.1177/107385840527745
9. Jong LW et al (2008) Strongly reduced volumes of putamen and thalamus in Alzheimer's disease: an MRI study. *Brain* 131:3277–3285
10. Llinas RR (1988) The intrinsic electrophysiological properties of mammalian neurons: insights into central nervous system function. *Science* 242:1654–1664
11. Lopes da Silva FH (1991) Neural mechanisms underlying brain waves: from neural membranes to networks. *Elec Clin Neurophysiol* 79:81–93
12. Lopes da Silva FH et al (1973) Model of brain rhythmic activity. *Kybernetik* 15:27–37
13. McCormick DA, Bal T (1997) Sleep and arousal: thalamocortical mechanisms. *Ann Rev Neurosci* 20:185–215
14. Niedermeyer E (1997) Alpha rhythms as physiological and abnormal phenomena. *Int Jour Psychophysiol* 26:31–49
15. Niedermeyer E, Lopes da Silva FH (1999) Electroencephalography: basic principles, clinical applications and related fields. Williams and Wilkins, Baltimore
16. Prinz PN, Vitiello MV (1989) Dominant occipital (alpha) rhythm frequency in early stage Alzheimer's disease and depression. *Elec Clin Neurophysiol* 73:427–432
17. Raji CA et al (2009) Age, Alzheimer disease, and brain structure. *Neurol* 73:1899–1905
18. Rissman RA et al (2007) *GABA_A* receptors in aging and Alzheimer's disease. *J Neurochem* 103:1285–1292
19. Rossini PM et al (2006) Conversion from mild cognitive impairment to Alzheimer's disease is predicted by sources and coherence of brain electroencephalography rhythms. *Neurosci* 143:793–803
20. Soininen H et al (1992) Slowing of electroencephalogram and choline acetyltransferase activity in post mortem frontal cortex in definite Alzheimer's disease. *Neurosci* 49(3):529–535
21. Stam CJ et al (1999) Dynamics of the human alpha rhythm: evidence for non-linearity? *Clin Neurophysiol* 110:1801–1813
22. Steriade M, Deschenes M (1984) The thalamus as a neuronal oscillator. *Brain Res Rev* 8:1–63
23. Suffczynski P (2000) Neural dynamics underlying brain thalamic oscillations investigated with computational models. *Inst Exp Phys, Uni Warsaw*
24. Tombol T (1967) Short neurons and their synaptic relations in the specific thalamic nuclei. *Brain Res* 3:307–326
25. Wilson HR, Cowan JD (1972) Excitatory and inhibitory interaction in localized populations of model neurons. *Jour Biophys* 12:1–23
26. Zetterberg LH et al (1978) Performance of a model for a local neuron population. *Biol Cyber* 31:15–26